

PARAMETERS FOR 1 TEV² P-P STORAGE RINGS

L. C. Teng

February 13, 1974

Preliminary parameters for 1 TeV² proton storage rings are given here. It is hoped that they can serve as the starting point for a design study.

A. Size and Layout

On the NAL site two different sizes are possible depending on whether the storage rings encircle the main ring. These two arrangements are shown in Fig. 1. The parameters will be developed below, but roughly the large rings encircling the main ring have a radius of ~2.5 km and the small rings have a radius of ~1.3 km. The advantages of the large rings over the small ones are:

1. The dipole field of the large rings is lower, being ~35 kG at 1 TeV compared to ~45 kG for the small rings. It is therefore possible to extend the large rings to higher energies, e.g. 2 TeV for a dipole field of ~70 kG.

2. The interaction straight sections of the large rings are much longer (~ 1000 m) than those of the smaller rings (~250 m). The longer straight sections offer greater flexibility for installing special function insertions to obtain beam characteristics appropriate for individual experiments. It is even possible to accommodate more than one experiment in a 1000 m straight section. The 250 m straight sections are rather too short. We will see later that for the small rings it is possible

and most desirable to extend two of the straight sections.

3. The geometry of the large rings encircling the main ring is such that a 1-TeV beam extracted from one of the rings can be transported to go down the present external beam line. Hence this ring can be used as a beam-spill stretcher for the 1-TeV energy doubler. This is most useful in view of the rather low pulse rate of the doubler.

The disadvantages of the large rings are:

a. It takes about twice as many pulses from the doubler to fill the large rings compared to the small rings.

b. Most importantly, the large rings will cost about twice as much as the small rings.

In the sections below we will develop the parameters for both the large and the small rings but will concentrate more explicitly on the small rings.

B. Ring Lattice

The ring lattice is developed on the basis of the following considerations:

1. The number of beam interacting straight sections (working part of the rings) should be large. We assume 8 straight sections joined together by eight 45" curved sections.

2. We assume the two rings to be located one on top of the other. The two oppositely circulating beams are brought vertically together in straight sections to collide with each other.

3. The most economical normal cell is the FODO cell, and the most advantageous phase advance per cell for the placement of beam manipulating elements is 90° . The amplitude function β , hence the transverse beam size, will then depend only on the

cell length L . If we want to maintain the doubler beam size as it is injected into the storage ring the value of β_{\max} in the storage ring should be about the same as that in the energy doubler, namely about 100 m. This gives a cell length of $L \approx 60$ m. Using the thin-lens approximation, for a phase advance per cell of 90° we get

$$\left\{ \begin{array}{l} L = 60 \text{ m} \\ \beta_{\max} = \left(1 + \frac{1}{\sqrt{2}}\right) L = 102.4 \text{ m} \\ \beta_{\min} = \left(1 - \frac{1}{\sqrt{2}}\right) L = 17.57 \text{ m} \\ k = \frac{B' \ell_Q}{(B\rho)} = 2\sqrt{2}/L = 0.04714 \text{ m}^{-1} \end{array} \right. \quad (1)$$

or $B' \ell_Q = 1574 \text{ kG}$ for $B\rho = 33388 \text{ kGm}$ (1 TeV)

4. A quadrupole used commonly by both beams has opposite focal actions on the two oppositely circulating beams. To facilitate the design of matched insertions in the straight sections all pairs of corresponding quadrupoles in the two rings should have opposite focal actions on the two beams, hence the same field-gradient polarity. To make the two rings identical in focusing sequence for the two beams a curved section should have an odd number of half normal cells.

5. Without specific insertions designated for the straight sections or during the initial commissioning of the rings the straight sections can be bridged across by normal cells with dipoles left out (straight cells). Since the phase advance per cell is 90° an integral multiple of 4 straight cells will match both optics and dispersion.

6. For the small rings, because of the constraint of the site, we have to push for higher fields. We assume a dipole field of ~ 45 kG and a quadrupole field gradient of ~ 900 kG/m, each being about twice that attainable in conventional Fe-Cu magnets. Also the convenient length of each dipole is ~ 6 m. A bit of cutting and fitting then gives the following parameters for the small rings.

$$\left\{ \begin{array}{l} n_Q = 2 = \text{No. of quadrupoles per cell (one F and one D)} \\ l_Q = 1.8 \text{ m} = \text{length per quadrupole} \\ B' = 874.4 \text{ kG/m} \end{array} \right.$$

$$\left\{ \begin{array}{l} n_B = 8 = \text{No. of dipoles per cell} \\ l_B = 5.9 \text{ m} = \text{length per dipole} \\ B = 44.44 \text{ kG} \quad \rho = 751.2 \text{ m} \\ \theta_B = 7.854 \text{ mrad} = \text{bend angle per dipole} \end{array} \right.$$

$$\left\{ \begin{array}{l} N_c = 12\frac{1}{2} = \text{No. of cells per curved section} \\ L_c = 12.5 \times 60 \text{ m} = 750 \text{ m} = \text{length per curved section} \\ R_c = L_c / \frac{\pi}{4} = 954.9 \text{ m} = \text{radius of curved section} \end{array} \right.$$

$$\left\{ \begin{array}{l} N_s = 4 = \text{No. of cells per straight section} \\ L_s = 4 \times 60 \text{ m} = 240 \text{ m} = \text{length per straight section} \end{array} \right.$$

$$\left\{ \begin{array}{l} N_r = 8(N_s + N_c) = 132 = \text{No. of cells per ring} \\ L_r = 132 \times 60 \text{ m} = 7920 \text{ m} = \text{length per ring} \\ R_r = L_r / 2\pi = 1260.5 \text{ m} = \text{equivalent radius of ring} \end{array} \right.$$

$$\left\{ \begin{array}{l} N_B = 8N_c n_B = 800 = \text{No. of dipoles per ring} \\ N_Q = N_r n_Q = 264 = \text{No. of quadrupoles per ring} \end{array} \right.$$

$$\nu = \frac{1}{4} N_r = 33 = \text{betatron oscillation tune (trimmed to } 33\frac{1}{4}\text{)}$$

A half normal cell is shown in Fig. 2 and an octant of the double ring is shown in Fig. 3. There are 4 D-D and 4 F-F straight sections in each ring, and a D-D straight section in one ring always coincides with an F-F straight section in the other ring and vice versa.

7. For the large rings the field intensity can be reduced to allow future increase to higher energies. We assume a dipole field of ~35 kG and a quadrupole field gradient of ~700 kG/m. Cutting and fitting gives the following parameters for the large rings.

$$\begin{aligned} n_Q &= 2 & l_Q &= 2.3 \text{ m} & B' &= 684.3 \text{ kG/m} \\ \left\{ \begin{array}{l} n_B = 8 \\ \theta_B = 5.950 \text{ mrad} \end{array} \right. & & l_B &= 5.8 \text{ m} & B &= 34.25 \text{ kG} \\ & & & & \rho &= 974.8 \text{ m} \\ \left\{ \begin{array}{l} N_c = 16\frac{1}{2} \\ R_c = L_c / \frac{\pi}{4} = 1260.5 \text{ m} \end{array} \right. & & L_c &= 16.5 \times 60 \text{ m} = 990 \text{ m} \\ N_s &= 16 & L_s &= 16 \times 60 \text{ m} = 960 \text{ m} \\ \left\{ \begin{array}{l} N_r = 8(N_s + N_c) = 260 \\ R_r = L_r / 2\pi = 2482.8 \text{ m} \end{array} \right. & & L_r &= 260 \times 60 \text{ m} = 15600 \text{ m} \\ N_B &= 8N_c \quad n_B = 1056 & N_Q &= N_r \quad n_Q = 520 \\ \nu &= \frac{1}{4} N_r = 65 \text{ (trimmed to } 65\frac{1}{4}\text{)} \end{aligned}$$

Again, a half normal cell is shown in Fig. 2, and an octant of the double ring is shown in Fig. 3.

8. In Fig. 4 we show the layout of two modified configurations of small rings with 2 of the 8 straight sections (IV and VIII)

lengthened to 720 m (12 straight cells) and to 960 m (16 straight cells). The 960 m straight-section rings can barely be shoehorned in with tunneling under the bubble chamber complex. We may have to settle for the 720 m straight-section rings. The modified lattice parameters are:

Small Rings-720

$$\begin{cases} N_{s1}(\text{short}) = 4 & L_s(\text{short}) = 4 \times 60 \text{ m} = 240 \text{ m} \\ N_{s2}(\text{long}) = 12 & L_{s2}(\text{long}) = 12 \times 60 \text{ m} = 720 \text{ m} \end{cases}$$

$$\begin{cases} N_r = 8N_c + 6N_{s1} + 2N_{s2} = 148 \\ L_r = 148 \times 60 \text{ m} = 8880 \text{ m} \\ R_r = L_r/2\pi = 1413.3 \text{ m} \end{cases}$$

$$N_Q = N_r n_Q = 296$$

$$\nu = \frac{1}{4} N_r = 37 \text{ (trimmed to } 37\frac{1}{4}\text{)}$$

Small Rings-960

$$\begin{cases} N_{s1}(\text{short}) = 4 & L_{s1}(\text{short}) = 4 \times 60 \text{ m} = 240 \text{ m} \\ N_{s2}(\text{long}) = 16 & L_{s2}(\text{long}) = 16 \times 60 \text{ m} = 960 \text{ m} \end{cases}$$

$$\begin{cases} N_r = 8N_c + 6N_{s1} + 2N_{s2} = 156 \\ L_r = 156 \times 60 \text{ m} = 9360 \text{ m} \\ R_r = L_r/2\pi = 1489.7 \text{ m} \end{cases}$$

$$N_Q = N_r n_Q = 312$$

$$\nu = \frac{1}{4} N_r = 39 \text{ (trimmed to } 39\frac{1}{4}\text{)}$$

9. Using the thin-lens and thin-bend approximation the extreme values of the dispersion function η (or x_p) for a

curved normal cell are

$$\begin{cases} \eta_{\max} = (4 + \sqrt{2}) L\theta_B \\ \eta_{\min} = (4 - \sqrt{2}) L\theta_B \end{cases} \quad (2)$$

It is expected that all special function insertions in the straight section will be designed to match the dispersion function η as well as the amplitude function β . Without any insertion (straight sections bridged by normal straight cells) the transition energy γ_t for a ring is given by

$$\gamma_t^2 = \frac{1}{28\theta_B^2} \left(\frac{N_r}{8N_c} \right) \quad (3)$$

For the various storage rings these formulas give

	$\eta_{\max}(\text{m})$	$\eta_{\min}(\text{m})$	γ_t	ν
Large ring	1.93	0.923	44.58	65 (65 $\frac{1}{4}$)
Small rings	2.55	1.22	27.65	33 (33 $\frac{1}{4}$)
Small ring-720	2.55	1.22	29.27	37 (37 $\frac{1}{4}$)
Small ring-960	2.55	1.22	30.05	39 (39 $\frac{1}{4}$)

where in the last column the values of the betatron tune are repeated for reference. The matched insertions will modify ν and γ_t but will not affect β and η in the curved sections.

10. All of these parameters will have to be trimmed slightly when the beam stacking process is taken into consideration.

C. Injection

As shown in Figs. 1 and 4 the transport lines to transport

the beams from the energy doubler to the various storage rings are:

1. Injection into Large Rings

	<u>Clockwise</u>	<u>Counterclockwise</u>
From - to	E0-VII	C0-V
Straight length (m)	500	200
Curved length (m)[angle]	450 [-26°]	2150 [123°]
Total length (m)	950	2350

2. Injection into Small Rings

	<u>Clockwise</u>	<u>Counterclockwise</u>
From - to	A0-I (Present Beam to Q-stub)	B0-VII
Straight length (m)	-	240
Curved length (m)[angle]	- [-8°]	560 [-32°]
Total length (m)	2450	800

3. Injection into Small Rings-720

	<u>Clockwise</u>	<u>Counterclockwise</u>
From - to	A0-I (Present beam to bubble chambers)	B0-VII
Straight length (m)	-	180
Curved length (m) [angle]	- [-11°]	710 [-41°]
Total length (m)	2680	890

4. Injection into Small Rings-960

	<u>Clockwise</u>	<u>Counterclockwise</u>
From - to	A0-I (Present beam to bubble chambers)	B0-VII
Straight length (m)	2690	180
Curved length (m)[angle]	190 [-11°]	710 [-41°]

	<u>Clockwise</u>	<u>Counterclockwise</u>
Total length (m)	2800	890
5. Extracted Beam from Large Ring		
	<u>Clockwise</u>	
From - to	VII-A0	
Straight length (m)	190	
Curved length (m)[angle]	1630 [-93°]	
Total length (m)	1820	

The beam extracted from the large clockwise ring and going back to A0 is used when the storage ring is operated as a beam-spill stretcher. The curved sections of the transports for injection into small rings-750 and small rings-960 can be housed in either the main-ring tunnel or the storage-ring tunnel. The radius of all the curved transport sections is assumed to be 1000 m, but clearly any lattice with a radius smaller than 1000 m can be used. Thus, we can use either the energy-doubler cells (radius \cong 915 m) or the small storage-ring cells (radius \cong 955 m). The straight transport sections will, again, consist of the same cells with dipoles left out. Matching quadrupoles will be used at either end of a beam transport line to match the optics and the dispersion. Fast extraction systems will be used to extract the beam in one turn from the doubler.

The beam is injected horizontally onto the injection orbit of the storage ring by magnetic septa and kickers. The phase advance of 90° between β_{\max} locations in normal straight cells is appropriate for the separation between the septa and the kickers. But the rather large positive slope of the β -function leading to β_{\max} requires a positive injection angle which, although obtainable,

is inconvenient. We can replace the 4 cells in the injection straight section by an insertion. The insertion should contain two high β locations P_1 (upstream) and P_2 (downstream) with a nearly parallel-to-point optics from P_1 to P_2 . The total phase advance across the insertion should still be 360° for matching dispersion. An example has been worked out. The part of the insertion relevant to the injection geometry is shown in Fig. 5. The horizontal transfer matrix from P_1 to P_2 is $\begin{pmatrix} 0.233 & 111.6 \text{ m} \\ -1/162.0 \text{ m} & 1.336 \end{pmatrix}$. Two slow pulsed magnetic septa will bring the horizontal position-slope vector off the beam to $\begin{pmatrix} 16.0 \text{ mm} \\ -0.0334 \text{ mrad} \end{pmatrix}$ at P_1 which, then, transfers to $\begin{pmatrix} 0 \\ -0.143 \text{ mrad} \end{pmatrix}$ at P_2 . A set of kickers at P_2 will kick the beam 0.143 mrad to follow the injection orbit.

Even for the small rings the injected beam fills only ~80% of the ring leaving a 5.5 μsec gap. Thus only a relatively slow kicker with a fall time of ~5 μsec is required. Such kickers can be made with laminated (~1 mil) iron core and pulsed to, say, 1 kG. A total of ~5 m length of kickers will be able to kick the 1-TeV beam 0.143 mrad. The kickers should have a small C-shaped aperture. They enclose and kick only the newly injected beam. A conducting screen which covers the opening of the C aperture and shields the kicker field from the stacked beam will open up after injection to allow the stacking rf to decelerate the injected beam out of the kicker and onto the beam stack.

The parameters of the magnetics (current) septa are, for example:

	<u>Septum 1</u>	<u>Septum 2</u>
Thickness	1.5 cm	0.5 cm
Current density	9550 A/cm ²	9550 A/cm ²

	<u>Septum 1</u>	<u>Septum 2</u>	
Field	18 kG	6 kG	
Length	12 m	12 m	
Separation	0.5 m		
Deflection angle	6.4695 mrad	2.1565 mrad	
Displacement- angle vector	entrance	$\begin{pmatrix} 95.5 \text{ mm} \\ -8.6594 \text{ mrad} \end{pmatrix}$	$\begin{pmatrix} 29.3 \text{ mm} \\ -2.1899 \text{ mrad} \end{pmatrix}$
	exit	$\begin{pmatrix} 30.4 \text{ mm} \\ -2.1899 \text{ mrad} \end{pmatrix}$	$\begin{pmatrix} 16.0 \text{ mm} \\ -.0334 \text{ mrad} \end{pmatrix}$

The geometry of the beam is also shown in Fig. 5.

D. Beam Stacking

Here we will use as an example only the case of the small rings. The beam is fast extracted from partially debunched stationary rf buckets on the flat-top of the energy doubler and captured at injection into properly matched and phased stationary rf buckets in the storage ring. After the kicker screen is opened the storage ring rf will decelerate the beam adiabatically out of the kicker and onto the beam stack.

1. The harmonic number of the rf in the main ring is 1113 at an equivalent radius of 1000 m. Hence the harmonic number of the doubler must be 1112 at an equivalent radius of 999.1015 m. At injection the frequencies of the doubler rf and the storage-ring rf must be identical, and not counting the beam transit time in the transport, the rf in the two machines must be in phase. The harmonic number of the storage ring should, therefore, be $h = 1403$ at the injection radius of $R = 1260.557$ m.

2. We shall see later that it is adequate to place the innermost (first) stacking orbit at an equivalent radius of 1260.537 m, or at $\Delta R = - 2.0$ cm inward from the injection orbit. To stack in this orbit the injected beam must be decelerated by ΔE given by

$$\frac{\Delta E}{E} = \gamma_t^2 \frac{\Delta R}{R} = - (27.65)^2 \frac{0.02}{1260.56} = - 0.01213 \quad (4)$$

or with $E = 1001$ GeV,

$$\Delta E = - 12.14 \text{ GeV.}$$

(Throughout this section we shall use the very good approximation $\frac{v}{c} = 1$ for 1-TeV protons.) We assume that this deceleration takes ~ 6 sec (~ -2 GeV/sec) at a synchronous phase angle of $\phi_s = - 60^\circ$. For this we need a peak rf voltage of $V = 60$ kV. This gives a deceleration rate of $(60 \text{ keV}) \sin(-60^\circ) = - 52.0 \text{ keV/turn}$. Since the proton revolution frequency is $\frac{c}{2\pi R} = 37.8 \text{ kHz}$ this corresponds to a deceleration rate of $- 52.0 \times 37.8 \text{ GeV/sec} = - 1.967 \text{ GeV/sec}$.

3. The half phase-width $\delta\phi$ of a stationary bucket is π and the half energy-width δE is given by

$$\delta E = E \left(\frac{2}{\pi h \Lambda} \frac{eV}{E} \right)^{1/2} \quad (5)$$

with

$$\Lambda \equiv \frac{1}{\gamma_t^2} - \frac{1}{\gamma^2} \quad .$$

The $\delta\phi \cdot \delta E$ area of the stationary bucket is

$$A = 8(\delta E). \quad (6)$$

The area of an accelerating (or decelerating) bucket is $A\alpha$ where $\alpha = \alpha(\phi_s)$ is tabulated e.g. in CERN/MPS - SI/Int. DL/70/4 (April 1970). For $h = 1403$, $V = 60$ kV, $\gamma_t = 27.65$, $\gamma = 1067$, and $\alpha(-60^\circ) = 0.059$ we get

$$\left\{ \begin{array}{l} \delta E = 0.144 \text{ GeV} \\ A = 1.15 \text{ GeV} \\ A\alpha = 0.068 \text{ GeV.} \end{array} \right.$$

Both the stationary bucket area of 1.15 GeV (for initial synchronous capture) and the decelerating bucket area of 0.068 GeV are adequate for the beam which has a bunch area in the $\delta\phi \cdot \delta E$ phase-space of only 0.033 GeV (corresponding to $\delta\phi \cdot \delta w$ phase-space area of 0.1 eV-sec obtained from measurement at 300 GeV in the main ring).

The rf voltage should be adiabatically dropped to 56 kV, hence ϕ_s shifted correspondingly to -67° before the beam bunches are moved onto the edge of the beam stack and the rf is turned off abruptly at the proper frequency. The reduced rf voltage gives a bucket area equal to the phase area of the beam bunch so that when the full buckets are moved into the stack and dumped the stack is not diluted in density.

Also since only 1112 of the 1403 buckets are filled with protons the remaining 291 empty buckets if allowed to enter the beam stack will dilute the stack density. These empty buckets should be suppressed. Thus the rf should be on during the 1112 cycles when there is beam, off during the next 291 cycles when there is no beam, on again during the next 1112 cycles etc.

4. The rf frequency for the injection orbit is

$$f = \frac{hc}{2\pi R} = 53.10508 \text{ MHz} \quad (\text{to accuracy } \frac{v}{c} = 1). \quad (7)$$

For the innermost stacking orbit

$$\frac{\Delta f}{f} = - \Lambda \frac{\Delta E}{E} = - \Lambda \gamma_t^2 \frac{\Delta R}{R} = 1.586 \times 10^{-5} \quad (8)$$

or

$$\Delta f = 842 \text{ Hz} .$$

The rate of frequency modulation is given by

$$\dot{f} = - \frac{\Lambda}{h} \frac{f^2}{E} \frac{dE}{dn} = 136.4 \text{ Hz/sec} \quad (9)$$

where $\frac{dE}{dn} = - 52 \text{ keV/turn} = \text{deceleration per turn}$. The total frequency swing of $\Delta f = 842 \text{ Hz}$ is reached in $\Delta t = \frac{842}{136.4} \text{ sec} = 6.17 \text{ sec}$ corresponding to a total deceleration of 12.14 GeV.

At the moment of stacking the half energy-width of the full bucket is 0.139 GeV. The beam should be deposited at an energy accuracy of the same order, namely $\delta E \pm 0.14 \text{ GeV}$ or $\frac{\delta E}{E} \sim \pm 1.4 \times 10^{-4}$. The turn-off (stacking) frequency of the rf should, then, be held accurate to

$$\frac{\delta f}{f} = - \Lambda \frac{\delta E}{E} \sim \pm 1.8 \times 10^{-7} \quad (10)$$

or

$$\delta f \sim \pm 10 \text{ Hz} .$$

5. We should check that the phase oscillation frequency during deceleration is high enough so that variation of parameters such as the rf voltage and frequency can be made adiabatically. The phase oscillation wave-number ν_s is given by

(for $\frac{V}{c} = 1$)

$$v_s = \left(\frac{h\lambda}{2\pi} \frac{eV}{E} \cos\phi_s \right)^{1/2} . \quad (11)$$

At $V = 60$ kV, $\phi_s = -60^\circ$ this gives

$$v_s = 0.935 \times 10^{-4} \quad \text{or} \quad f_s = v_s \frac{c}{2\pi R} = 3.54 \text{ Hz}$$

and at $V = 56$ kV, $\phi_s = -67^\circ$ this gives

$$v_s = 0.799 \times 10^{-4} \quad \text{or} \quad f_s = v_s \frac{c}{2\pi R} = 3.02 \text{ Hz} .$$

Although these are very slow oscillations, they are fast enough compared to the total deceleration time of ~ 6 sec.

6. For proper beam-bunch shape matching during the transfer from the doubler to the storage ring the stationary rf buckets in the two machines must have identical energy-widths. The half energy-width of the buckets in the storage ring is $\delta E = 0.144$ GeV. In order that the buckets in the doubler ($h = 1112$, $\gamma_t = 18.6$) have the same δE the peak rf voltage should be

$$V_D = 105.1 \text{ kV} .$$

This can be supplied by a single rf cavity.

To summarize the entire stacking procedure: on the flat-top of the doubler the rf voltage is first reduced adiabatically to $V_D = 105.1$ kV. The 1112 beam bunches are then fast extracted, transported, and injected into the storage ring. The shielding screen of the injection kicker should be closed at

injection. At injection the storage ring rf has a constant voltage of 60 kV and a constant frequency equal to that of the doubler rf, and is phased so that the beam bunches fall on $\phi_s = 0$. The beam bunches are, thus, captured into 1112 matched stationary rf buckets with an area some 35 times the bunch area - the remaining 291 rf buckets are suppressed. After injection the kicker screen is opened and the rf frequency is modulated at a rate of $\dot{f} = 136.4$ Hz/sec. This decelerates the beam out of the kicker onto the stack at a rate of $\dot{E} = -1.967$ GeV/sec. For an rf voltage of 60 kV the synchronous phase is $\phi_s = -60^\circ$ and the area of the decelerating bucket is about twice the bunch area. In the meantime the rf voltage is slowly reduced to 56 kV, the rate of frequency modulation being maintained. This shifts the synchronous phase to $\phi_s = -67^\circ$ and reduces the bucket area to exactly equal the bunch area. The rf is turned off abruptly when its frequency reaches that corresponding to the edge of the beam stack. The rf turn-off frequency should be accurate to ± 10 Hz. With careful manipulation the stacking efficiency $\equiv \frac{\text{density in stack}}{\text{density in bunch at injection}}$ can be high as 80%.

E. Aperture

The aperture requirements in straight sections depend on the special-function insertions and have to be examined individually. Here we can study only the general requirements in curved sections where the amplitude and dispersion functions are not affected by matched insertions in straight sections.

1. The largest horizontal aperture requirement occurs at F quadrupoles where horizontal β and η have their maximum values:

$$\begin{cases} \beta_{\max} = 102.4 \text{ m} \\ \eta_{\max} = 2.55 \text{ m} . \end{cases}$$

The separation between the injection orbit and the innermost stacking orbit assumed in Section D is expressed in:

$$\begin{cases} \text{difference in equivalent radius} = \Delta R = - 20 \text{ mm} \\ \text{difference in energy} = \frac{\Delta E}{E} = - 0.01213 . \end{cases}$$

At an F quadrupole the horizontal separation between these two orbits is, therefore

$$\Delta x = \eta_{\max} \frac{\Delta E}{E} = - 31 \text{ mm} . \quad (12)$$

The present full horizontal beam size at β_{\max} in the main ring is ~ 4 mm at 300 GeV. With multiturn injection into the booster one may expect the beam size to increase to ~ 10 mm at 300 GeV or ~ 6 mm at 1000 GeV. With our orbit radius of $\rho = 751.2$ m in a 5.8 m long dipole the sagitta is ~ 6 mm. Hence the minimum good field width should be

$$31 \text{ mm} + 6 \text{ mm} + 6 \text{ mm} = 43 \text{ mm}.$$

With some safety allowance we will want a

$$\text{Horizontal good field width} = 50 \text{ mm}.$$

Adding 15 mm on each side for poor field region we get a

$$\text{Horizontal coil aperture} = 80 \text{ mm}.$$

This is shown in full scale in Fig. 6.

2. In Fig. 6 we show a geometrical beam-stack width between the innermost and the outermost stacking orbits of

$\hat{\delta}x = 10$ mm. This corresponds to an energy width of

$$\frac{\hat{\delta}E}{E} = \frac{\hat{\delta}x}{\eta_{\max}} = 3.92 \times 10^{-3}$$

or

$$\hat{\delta}E = 3.93 \text{ GeV}$$

or a $\delta\phi \cdot \delta E$ phase-space area of $2\pi\hat{\delta}E = 24.7$ GeV. With 80% stacking efficiency and a beam bunch area of 0.033 GeV this stack can accommodate

$$\frac{24.7}{0.033} \times 80\% \approx 600 \text{ (ignoring difference in radii)}$$

turns from the doubler. Even assuming the doubler current is only 40 mA, that now available from the main ring, we get a stack current of 24 A. Later we shall see that the beam-stack current is likely to be limited to < 24 A by other factors.

The frequency width of the full beam stack is given by

$$\frac{\hat{\delta}f}{f} = -\Lambda \frac{\hat{\delta}E}{E} = -5.13 \times 10^{-6}$$

or

$$\hat{\delta}f = -272 \text{ Hz} .$$

Thus, the frequency excursion from the injection orbit to the outermost (last) stacking orbit is $842 \text{ Hz} - 272 \text{ Hz} = 570 \text{ Hz}$. At the modulation rate of $\dot{f} = 136.4 \text{ Hz/sec}$ it takes 4.8 sec to decelerate the beam to the last stacking orbit.

3. The vertical aperture is determined by space-charge considerations. We shall see later in Section F that a vertical aperture of 50 mm as shown in Fig. 6 is adequate.

4. It is expected that all kinds of correction multipole magnets will be installed in the 3 m short straight sections to trim out closed-orbit distortions and low-order resonances (perhaps up to the 6th order). Initially the large uncorrected closed-orbit distortions will limit the effective good field aperture and the strong untrimmed low-order resonances will limit the useable tune spread. These effects and the initial poor vacuum will limit the beam current that can be stacked to a low value. As the field errors are corrected to higher precisions and the vacuum gets better the useable aperture and tune spread will enlarge and higher beam current can then be stacked.

F. Space-Charge Limits and Luminosity

For a continuous beam we shall consider only the transverse space-charge force. This force, if too large, will cause transverse instabilities. The space-charge force generally contains all nonlinear terms - terms proportional to all powers of the transverse displacement. However, for a given transverse distribution in the beam (generally a Gaussian) the ratios of all the nonlinear terms to the linear term are fixed and the space-charge effect can be quantified by a single parameter - the linear tune shift $\delta\nu$.

1. For a single beam the tune shift is caused by the self-force which depends on the cross-sectional configurations of the beam and the vacuum chamber surrounding the beam. We shall approximate the vacuum chamber by two parallel plates having infinite conductivity and permeability with an infinitely thin beam travelling half way in between, and calculate the tune

shift in the direction perpendicular to the plates. This gives a δv which may be too large by a factor of up to 5 and which should therefore be considered as a pessimistic upper limit. The result is

$$\delta v = - \frac{r_p}{32} \frac{1}{v\gamma} \left(\frac{2\pi R}{g} \right)^2 \frac{I}{ec} \quad (13)$$

where

$$\left\{ \begin{array}{l} r_p = \frac{e^2}{mc^2} = \text{proton radius} = 1.535 \times 10^{-18} \text{ m} \\ 2g = \text{separation between plates} \approx \text{vacuum chamber height} \\ I = \text{beam current} . \end{array} \right.$$

For the small rings $g = 0.025$ m, $2\pi R = 7920$ m, $v = 33$, $\gamma = 1067$, and we get

$$\delta v/I = - 0.00285 \text{ A}^{-1} .$$

The maximum beam current that can be stacked depends on the maximum allowable $|\delta v|$ without causing long-term transverse instabilities. The trouble is that we do not have a reliable value for the allowable $|\delta v|$. Various estimates based on semi-theory and rough measurements give values ranging from 0.05 to 0.25. Nevertheless, even the lower limit of $|\delta v| = .05$ gives a maximum attainable beam current of

$$I_{\max} = \frac{0.05}{0.00285} \text{ A} = 17.5 \text{ A} .$$

This shows that if our minimum goal of beam current is 10 A, $2g = 5$ cm is an appropriate choice for the vertical aperture of the ring.

2. When two beams collide the space-charge force of one

beam (subscript 2) will cause a tune shift in the other beam (subscript 1). The tune shift depends on the cross-sectional geometry of beam No. 2. We assume an elliptical cross-section with semi-major axis a_2 and semi-minor axis b_2 , and calculate δv in the direction of b_2 (the larger tune shift). The result is

$$\delta v_1 = \frac{2r_p}{\pi} \frac{\beta_1^*}{\gamma_1} \frac{\ell}{b_2(a_2+b_2)} \frac{I_2}{ec} \quad (14)$$

where

$$\begin{cases} \beta_1^* & = \text{amplitude function } \beta \text{ at collision point} \\ \ell & = \text{length over which the beams collide.} \end{cases}$$

We assume the beams to collide in a straight section insertion where the dispersion function η is made zero and where the amplitude function β^* is reduced to an extremely small value of, say, 1 m in both planes for both beams. The beam cross-sectional dimensions are

$$a_2 = 3 \text{ mm} \quad b_2 = 1.2 \text{ mm} \quad \text{at } \beta \sim 100 \text{ m}$$

or

$$a_2 = 0.3 \text{ mm} \quad b_2 = 0.12 \text{ mm} \quad \text{at } \beta \sim 1 \text{ m.}$$

These values give

$$\delta v_1 / \ell I_2 = - 0.000378 \text{ m}^{-1} \text{ A}^{-1} .$$

Too large a current of beam No. 2 and/or too long a collision region will cause too large a tune shift in beam No. 1 and make it unstable. Here again there is no reliable value for the maximum allowable $|\delta v|$. In this case because the tune shift

is produced locally within a short collision region, hence the δ -function like forces having much larger high harmonics tend to be more destructive, it is generally believed that the allowable value would range from 0.025 to 0.005, namely an order of magnitude lower than that for the single-beam tune shift. If we take the lower limit of $|\delta\nu| = 0.005$ we get

$$(\ell I_2)_{\max} = \frac{0.005}{0.000378} \text{ A-m} = 13.2 \text{ A-m} .$$

For a 1 m long collision region a current of 10 A is safe.

It should be remarked that we have taken here all the pessimistic lower limits. It is quite likely that much higher currents can in fact be stacked in these storage rings.

3. For two beams with identical cross-sectional area A^* colliding head-on over a length ℓ the luminosity L is given by

$$L = \frac{2c}{A^*} \left(\frac{I_1}{ec} \right) \left(\frac{I_2}{ec} \right) \ell . \quad (15)$$

For beams with non-uniform cross-sectional density distribution the effective area A^* must be calculated by evaluating an overlap integral. But for design purpose the value

$$A^* = \pi a_2 b_2 = 1.13 \times 10^{-3} \text{ cm}^2$$

gives a good enough approximation. Taking $\ell = 1 \text{ m}$ and $I_1 = I_2 = 10 \text{ A}$ we get

$$L = 2.3 \times 10^{34} \text{ cm}^{-2} \text{ sec}^{-1} \text{ (per collision region).}$$

To stack a 10 A beam in each ring using a 40 mA energy-doubler beam would take a total of $\frac{2 \times 10 \text{ A}}{0.04 \text{ A}} \cdot \frac{1260 \text{ m}}{1000 \text{ m}} = 630$ pulses. At a rate of 1 pulse per 100 sec this will take 63000 sec or $17\frac{1}{2}$ hours. Clearly some modifications of the doubler parameters must be made before these design values of beam-stack current and luminosity can be considered realistic.

G. Special-Function Insertions

The design concept and procedure for the special function insertions in straight sections together with a few examples for the large rings were described in FN-255 and will not be repeated here. It suffices to mention that all the insertions are mutually matched and modularized in length to integral multiples of half-cell length, and are, therefore, mutually replaceable and joinable with maximum flexibility. There are two general classes of insertions. Those in the first class modify the local beam characteristics to meet the requirements of individual experiments. Insertions of the second class are used to modify the integrated beam characteristics around the ring such as the tune ν and the transition energy γ_t for optimizing the performance of the ring especially after a change is made in insertions of the first class.

The examples worked out show that collision regions with zero dispersion and low- β values of 1 m in both planes are indeed feasible. They also indicate that 4-cell 240 m straight sections are too short and that to realize the flexibility inherent in this concept the length of a straight section must be at least 12 cells or 720 m. To use a 4-cell straight section one must, at the outset, have some specific experiment in mind

and design the insertion accordingly. Even then, one will suffer from the following drawbacks:

1. It is likely that substantial compromises must be made for each experiment between desired and obtainable beam characteristics.
2. The effect of the insertion will not be entirely local. We may have to contend with possible interferences between experiments in different straight sections.
3. The non-local effects of these insertions may degrade the performance of the storage ring as a whole.
4. To change experiments in a straight section will involve redesigning and rebuilding the insertion, each time retuning a "new" machine with different characteristics.

H. Acknowledgement

Many people participated in the discussion of 1 TeV² p-p storage rings during the 1973 NAL Summer Study at Aspen. Their ideas are used freely in this report. For their specific contributions the reader is referred to the forthcoming Report of the 1973 Aspen Summer Study.

It should be pointed out that the most serious problems of the parameters for the superconducting magnet system and the vacuum system were not studied at all here.

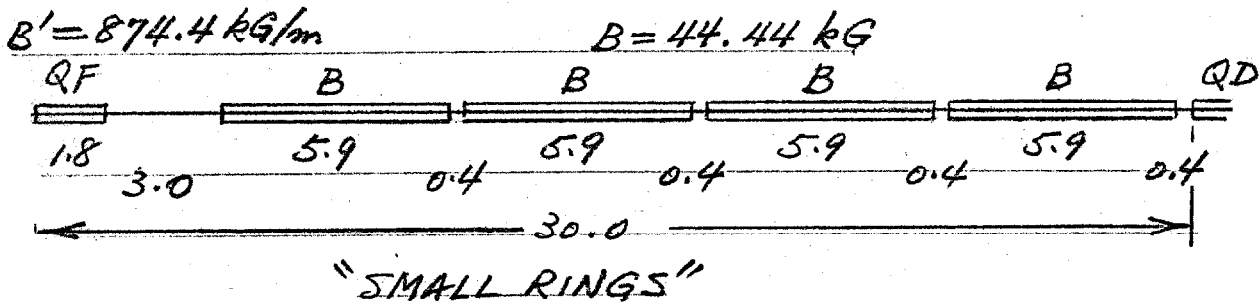
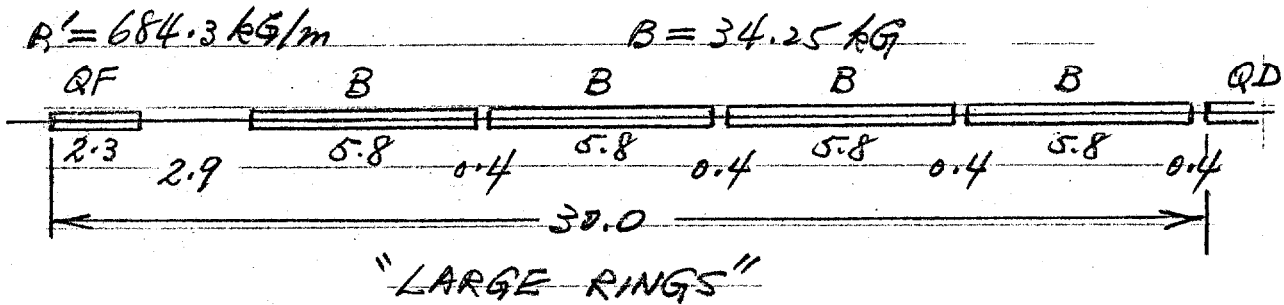


FIGURE 2 HALF NORMAL CELLS
(ALL LENGTHS IN METERS.)

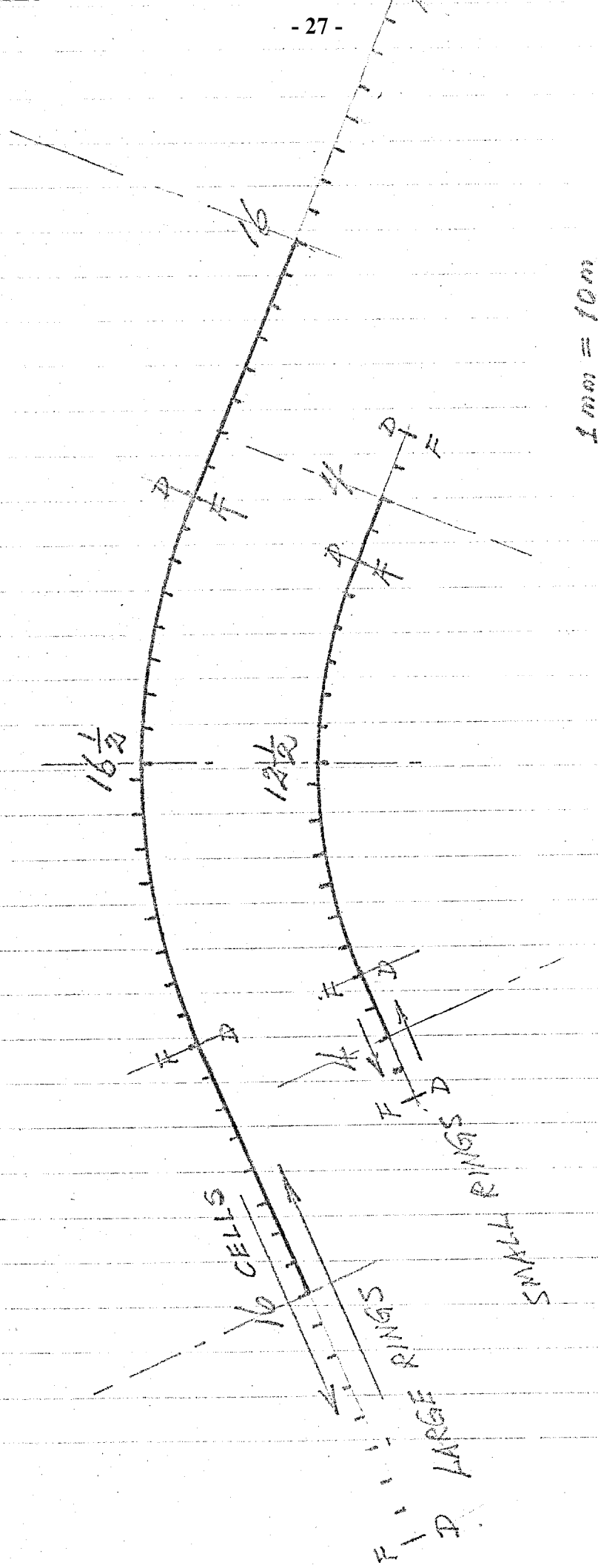


FIGURE 3 ONE SECTOR (OCTANT) OF THE RINGS

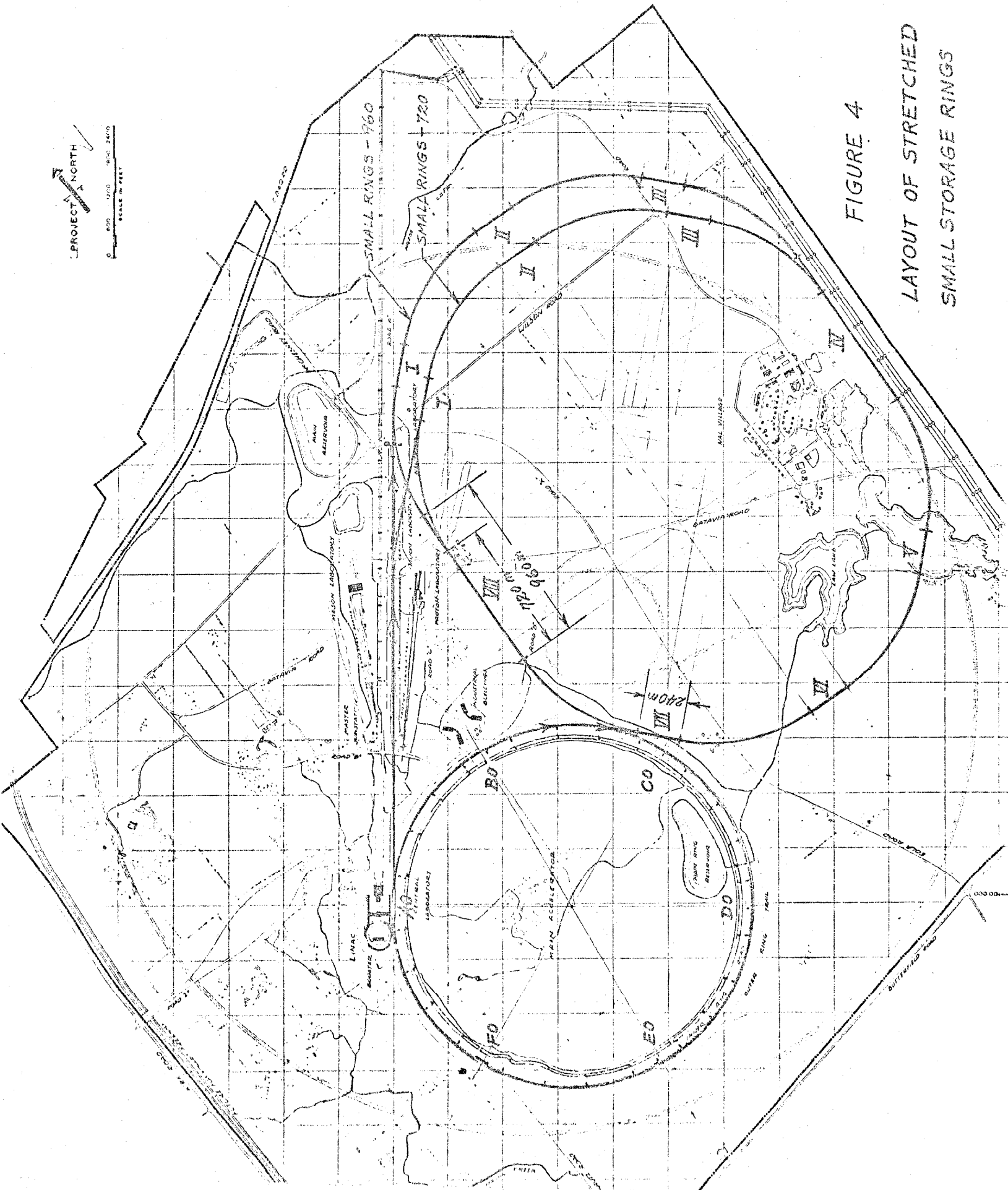


FIGURE 4
LAYOUT OF STRETCHED
SMALL STORAGE RINGS

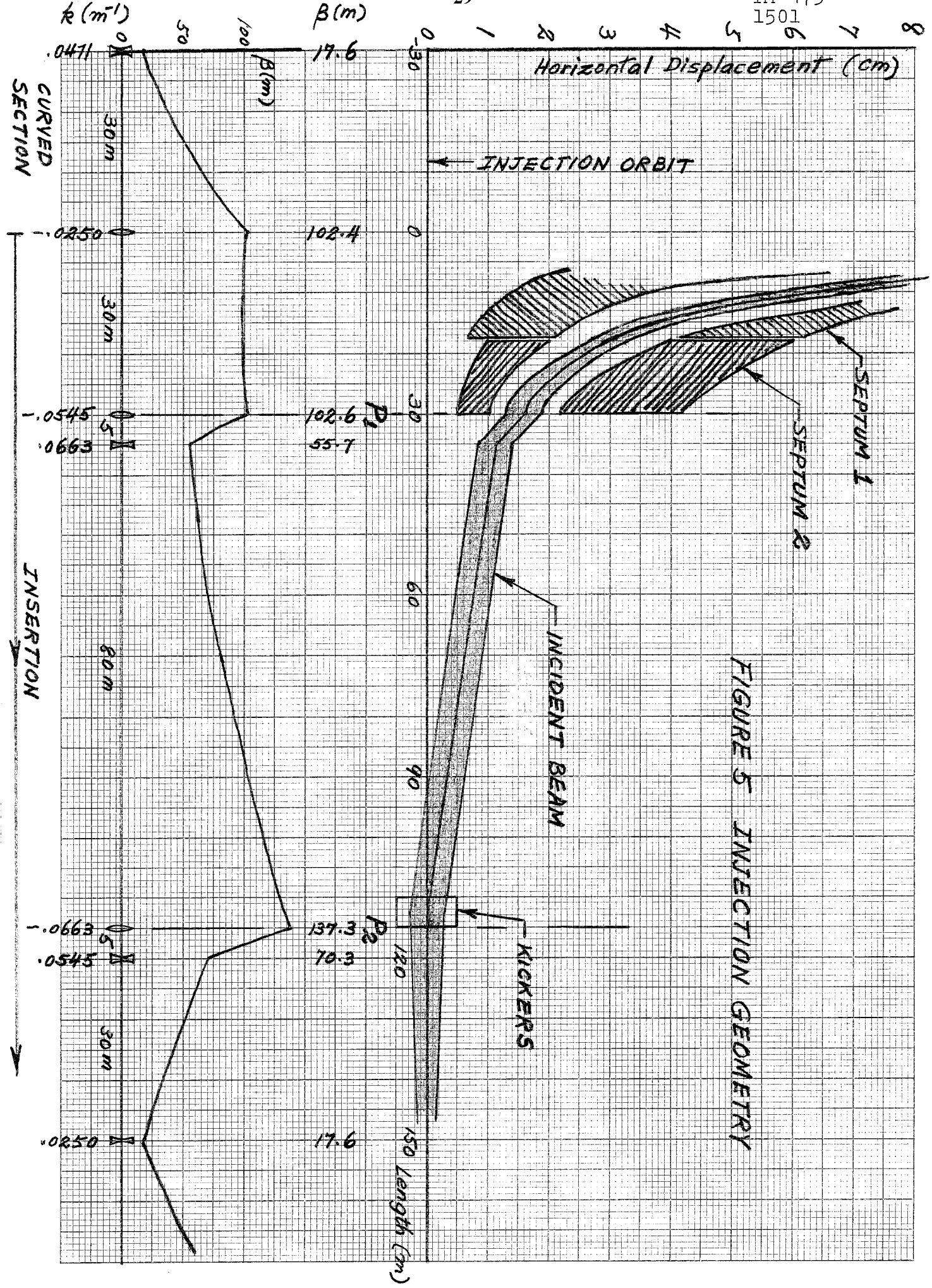


FIGURE 5 INJECTION GEOMETRY

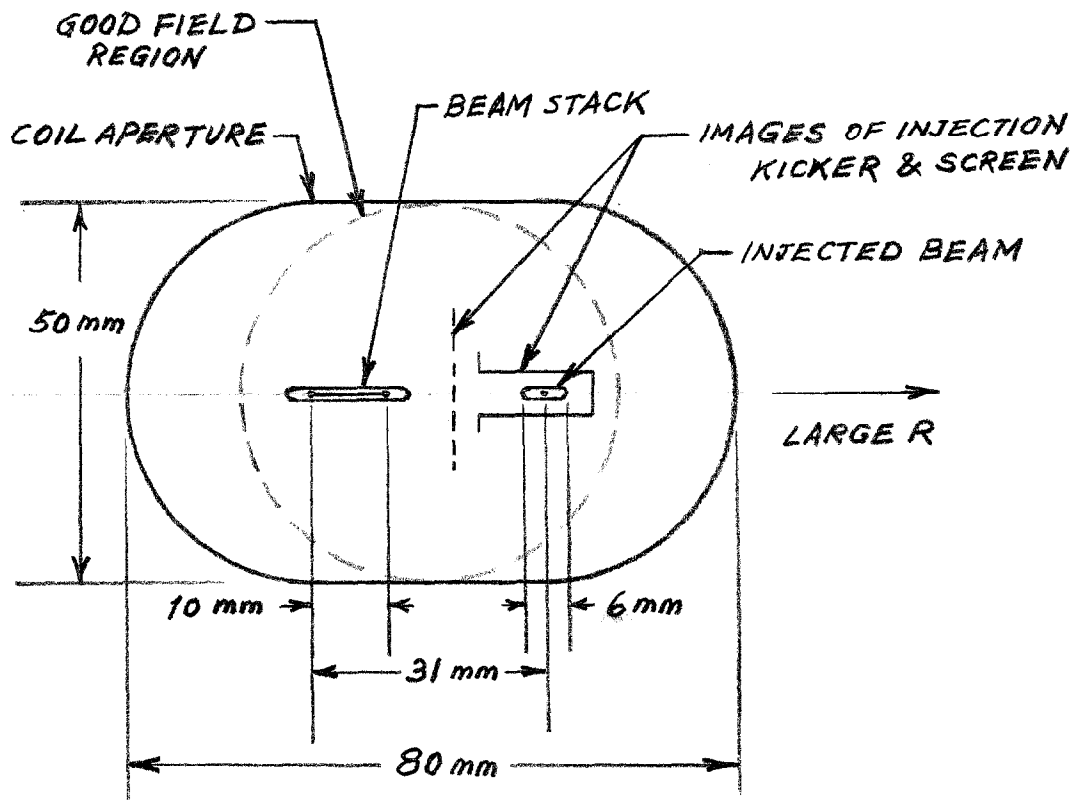


FIGURE 6 APERTURE AND STACKING
(FULL SCALE)